Theoretical investigation of finite size effects at DNA melting

Sahin Buyukdagli and Marc Joyeux*
Laboratoire de Spectrométrie Physique (CNRS UMR 5588), Université Joseph Fourier—Grenoble 1, Boîte Postale 87, 38402 St Martin d'Hères, France

(Received 6 March 2007; revised manuscript received 2 May 2007; published 17 August 2007)

We investigated how the finiteness of the length of a sequence affects the phase transition that takes place at the DNA melting temperature. For this purpose, we modified the transfer integral method to adapt it to the calculation of both extensive (partition function, entropy, specific heat, etc.) and nonextensive (order parameter and average separation between paired bases) thermodynamic quantities of finite sequences with open boundary conditions, and applied the modified procedure to two different dynamical models. We characterized in some detail the three effects that take place when the length of the sequence is decreased, namely, (i) the decrease of the critical temperature, (ii) the decrease of the peak values of all quantities that diverge at the thermodynamic limit but remain finite for finite sequences, like the specific heat and the correlation length, and (iii) the broadening of the temperature range over which the transition affects the dynamics of the system. We also performed a finite size scaling analysis of the two models and showed that the singular part of the free energy can indeed be expressed in terms of a homogeneous function. However, Josephson's identity is satisfied for none of the investigated models, so that the derivation of the characteristic exponents which appear, for example, in the expression of the specific heat requires some care.

DOI: 10.1103/PhysRevE.76.021917 PACS number(s): 87.14.Gg, 05.70.Jk, 87.15.Aa, 64.70.−p

I. INTRODUCTION

According to Ehrenfest's definition, small systems do not exhibit phase transitions. Indeed, instead of a sharp peak or a discontinuity at some well-defined temperature, systems with finite size show a more or less smooth hump extending over some finite range in the temperature evolution of the specific heat. In some sense, this broader feature can be considered as the finite system analog of a phase transition. This led Proykova and Berry, for example, to interpret a structural transition in TeF_6 clusters as a second-order phase transition [1]. Of course, the study of the dependence of the thermodynamic quantities on the size and/or the particle number of the system is the most common way to decide whether a transition in a finite system is the actual precursor of a phase transition in the corresponding infinite system [2]. However, some authors have tried to provide more formal definitions of phase transitions in finite systems, which are based on either the inspection of the shape of the calorimetric curve [3–5] or the density of complex zeros of the canonical partition function [6–9].

The melting of DNA sequences, that is, the separation of the two strands upon heating, is a phenomenon which lends itself quite naturally to the investigation of finite size effects because sequences with very different lengths, ranging from a few base pairs to tens of thousands of them, can be synthesized on demand. Investigation of the melting of DNA homopolymer pairs (i.e., of sequences whose strands are composed of a single type of base) turns out to be particularly enlightening, because it appears as a genuine first-order phase transition [10], while that of natural (inhomogeneous) sequences occurs in multiple steps and is highly sensitive to the details of the sequence [11,12]. It was recognized very early that the broadening of the transition upon decrease of the sequence length is accompanied by a decrease of the melting temperature (see, for example, Fig. 5 of Ref. [13]). Since that time, a similar behavior has also been observed in the melting of more complex systems, like polylactides [14] and hybrids of DNA and oxypeptide nucleic acids [15]. Semiempirical formulas, which are used, for example, by online oligonucleotide property calculators, generally consider that the melting temperature of a DNA sequence with N base pairs varies as $-820/N$ if $13 \leq N \leq 50$ and as $-500/N$ if $N > 50$. While slightly different relations are sometimes fitted against experiments [16], the $1/N$ dependence at large N is usually conserved.

The reasons that the evolution of the melting temperature as a function of the sequence length has been so thoroughly characterized are certainly that (i) the knowledge of the melting temperature is of practical and primary importance for many investigations, and (ii) the melting temperature is easily determined with all methods that are currently used to uncover the properties of DNA denaturation, like uv absorption spectroscopy around 260 nm, circular dichroism spectroscopy, differential scanning calorimetry [17,18], Raman spectroscopy [18], and electrophoretic mobility assays [19,20]. In addition, experimentalists also characterized the evolution of thermodynamic parameters as a function of the length of the sequence by differential calorimetry and uv absorption spectroscopy (see, for example, Refs. [17,21,22]), and investigated more specific points, like the persistency of intermediate states (i.e., metastable states with large bubbles) down to very short sequences with $13 \leq N \leq 48$ [23,24] (note that the ability of the models used in this work to display these metastable states is still subject to controversy [25,26]).

The purpose of the present work is to complete these experimental results by proposing a theoretical description of the melting transition of sequences with a finite number N of base pairs. The shift in the melting temperature will, of course, be discussed, but we also investigated the behavior

*Marc.JOYEUX@ujf-grenoble.fr

with decreasing N of extensive thermodynamic quantities, like the entropy and the specific heat, as well as the average separation between paired bases and the correlation length. These studies rely on two models which describe DNA sequences as one-dimensional chains. The first model is due to Dauxois, Peyrard, and Bishop (DPB) [27]. These authors showed that the introduction of an anharmonic contribution in the interaction term between successive base pairs, the effect of which is to lower this interaction at large separations of the paired bases, leads to a sharper and hence more realistic denaturation of the sequence than the model originally suggested by Peyrard and Bishop [28]. Joyeux and Buyukdagli (JB) [29] recently proposed an alternative model, which takes into account the fact that stacking enthalpies between successive base pairs are necessarily finite [30], and also displays a sharp first-order transition at the thermodynamic limit of infinitely long chains. Note that both the DPB and JB models can be extended to take into account additional (torsional) degrees of freedom [31,32] but that the simplest versions of the models have been considered in this study.

In Ref. [33] we used the transfer integral (TI) method [34,35] to investigate the critical properties of both the DPB and JB models, that is, to calculate the critical exponents at the thermodynamic limit and check the validity of the four scaling laws which connect the six fundamental exponents (see also Ref. [36] for an older attempt to evaluate the critical exponents). We showed that the Rushbrooke and Widom identities, which rely on the hypothesis that the free energy can be described by a single homogeneous function, are satisfied, while the Josephson and Fisher identities are not. We argued that this is probably due to the divergence of the average distance between paired bases at melting, which invalidates the assumption that the correlation length is solely responsible for singular contributions to thermodynamic quantities [33].

In the present work, we again used the TI method to estimate the temperature evolution of the entropy, the specific heat, the correlation length, and the average base pair separation for decreasing values of N. This, however, required substantial improvement of the procedure used in Ref. [33], because the latter is valid only at the thermodynamic limit of infinitely long chains. To this end, we extended the transfer matrix approach for open chains developed by Zhang *et al.* [35] to adapt it to the practical calculation of the correlation length and the average separation between paired bases. To get a better insight into the melting dynamics of finite sequences, we also checked to what extent these systems are amenable to finite size scaling analysis. Finite size scaling theory was developed by Fisher and Barber [37] in the early 1970s as a tool to analyze the volume dependence of critical phenomena and in particular the associated rounding of critical singularities and the shift in the critical point. It has also been used as an alternative way to determine the critical exponents that characterize a phase transition. Among the dozens of systems exhibiting first- or second-order phase transitions that have been studied by finite size scaling theory, let us mention the five- [38,39] and six-dimensional [40] Ising models and percolation models [41,42]. Like the derivation of the scaling laws, finite size scaling theory relies on some kind of homogeneity assumption. Since the validity of such assumptions was shown to be questionable in the case of infinitely long DNA sequences [33], it is necessary to check thoroughly their validity for finite size sequences.

The remainder of this paper is organized as follows. The DPB and JB models are briefly described in Sec. II, while the derivation of the TI formulas we used to calculate the thermodynamic properties of finite chains is sketched in Sec. III and the Appendix. Results dealing with the rounding of the DNA melting transition and the applicability of finite size scaling theory to this system are finally presented and discussed in Sec. IV.

II. NONLINEAR HAMILTONIAN MODELS FOR DNA

The Hamiltonians of the two DNA models whose critical behavior is studied in this paper are of the form

$$H = \sum_{n=1}^{N} \left\{ \frac{p_n^2}{2m} + V_M(y_n) + W(y_n, y_{n-1}) \right\}, \tag{1}$$

where y_n is the transverse stretching of the hydrogen bond between the nth pair of bases, while the one-particle Morse potential term

$$V_M(y_n) = D(1 - e^{-A_M y_n})^2 \tag{2}$$

models the binding energy of the hydrogen bond. The choice of the nearest-neighbor interaction potential $W(y_n, y_{n-1})$ is crucial, since the shape of the transition, which is a collective effect, depends primarily on its form. The DPB model [27] assumes that the stacking interaction between two successive base pairs is of the form

$$W(y_n, y_{n-1}) = \frac{K}{2}(y_n - y_{n-1})^2(1 + \rho e^{-\alpha(y_n + y_{n-1})}). \tag{3}$$

This nonlinear stacking interaction has the particularity of having a coupling constant which drops from $K(1+\rho)$ to K as the paired bases separate. This decreases the rigidity of the DNA chain close to the dissociation and yields a sharp, first-order transition.

The JB model [29] instead assumes that

$$W(y_n, y_{n-1}) = \frac{\Delta H}{2}(1 - e^{-b(y_n - y_{n-1})^2}) + K_b(y_n - y_{n-1})^2, \tag{4}$$

where the first term describes the finite stacking interaction and the second one the stiffness of the phosphate-sugar backbone. Note that the constant K_b that appears in Eq. (4) is 2000 times smaller than the harmonic coupling K of the DPB model and that one just needs to plug into Eq. (4) the stacking enthalpies ΔH determined from thermodynamic calculations [30] to describe inhomogeneous sequences.

Numerical values of the parameters used in this work are those of Refs. [29,36], that is, $D=0.03$ eV, $A_M=4.5$ Å^{-1}, $\alpha=0.35$ Å^{-1}, $K=0.06$ eV Å^{-2}, and $\rho=1$ for the DPB model, and $D=0.04$ eV, $A_M=4.45$ Å^{-1}, $\Delta H=0.44$ eV, $K_b=10^{-5}$ eV Å^{-2}, and $b=0.10$ Å^{-2} for the JB model.

III. TRANSFER INTEGRAL METHOD FOR FINITE CHAINS WITH OPEN BOUNDARY CONDITIONS

In order to correctly describe the DNA melting transition, one should take into account, in addition to the nonlinear Hamiltonians discussed in the previous section, the dissociation equilibrium $S_2 \leftrightarrow 2S$ which properly governs the separation of the two complementary strands (S) when the last base pair of double-stranded DNA (S_2) opens [11,43]. The $S_2 \leftrightarrow 2S$ equilibrium is generally ignored when calculating the partition function Z of all sequences except for "very short" ones close to the melting transition. The reason is that for sequences which are not too short the fraction of intact hydrogen bonds between complementary bases goes from 1 to almost 0 at the denaturation temperature without the two strands completely separating: the few remaining bonds indeed prevent the two strands from parting. In contrast, for very short sequences the processes of single bond disruption and strand dissociation take place in the same temperature range, so that inclusion of the $S_2 \leftrightarrow 2S$ equilibrium is essential to describe the melting transition correctly. The limit of very short sequences appears to lie around $N=100$ or 200 [44,45]. As a consequence, calculations aimed at determining nearest-neighbor stacking interactions from the melting temperatures of large sets of sequences containing fewer than 20 base pairs should take this equilibrium into account [46]. The $S_2 \leftrightarrow 2S$ equilibrium will, however, be disregarded in the present work, which focuses on sequences with $N \geq 100$ at temperatures smaller than the critical one.

The partition function Z of double-stranded DNA can be expressed as

$$Z = \int dy_1 dy_2 \cdots dy_N \exp\left(-\beta \sum_n [V_M(y_n) + W(y_n, y_{n-1})]\right), \tag{5}$$

where $\beta=(k_B T)^{-1}$ is the inverse temperature. The transfer integral method is a technique for efficiently computing Z. For this purpose, one first defines the TI kernel

$$K(y_n, y_{n-1}) = \exp\{-\beta[V_M(y_n)/2 + V_M(y_{n-1})/2 + W(y_n, y_{n-1})]\} \tag{6}$$

and expands it in an orthonormal basis

$$K(y_n, y_{n-1}) = \sum_i \lambda_i \Phi_i(y_n) \Phi_i(y_{n-1}), \tag{7}$$

where the $\{\Phi_i\}$ and $\{\lambda_i\}$ are the eigenvalues and eigenvectors of the integral operator and satisfy

$$\int dx\, K(x,y) \Phi_i(x) = \lambda_i \Phi_i(y). \tag{8}$$

For sequences with N base pairs and periodic boundary conditions ($y_N=y_0$), the partition function Z can be rewritten in the form

$$Z = \int dy_1 dy_2 \cdots dy_N \prod_{n=1}^{N} K(y_n, y_{n-1}). \tag{9}$$

By substituting the kernel expansion of Eq. (7) into Eq. (9), one gets

$$Z = \sum_i \lambda_i^N, \tag{10}$$

which at the thermodynamic limit of infinitely long chains ($N \to \infty$) reduces to $Z=\lambda_1^N$, where λ_1 is the largest eigenvalue of the integral operator. This simple expression of the partition function was used in Ref. [33] to calculate the critical exponents of infinitely long homogeneous DNA sequences at denaturation and check the validity of the associated scaling laws. For the sake of a safer comparison with real systems, the analysis below, however, deals with sequences with open boundary conditions, i.e., no special condition is imposed on the first and last base pairs of the sequence. Instead of Eq. (9), the partition function Z must be expressed in the form

$$Z = \int dy_1 dy_2 \cdots dy_N e^{-\beta V_M(y_1)/2} K(y_2, y_1) \times K(y_3, y_2) \cdots K(y_N, y_{N-1}) e^{-\beta V_M(y_N)/2}. \tag{11}$$

To evaluate this expression, let us introduce, as in Ref. [35],

$$a_i = \int dy\, e^{-\beta V_M(y)/2} \Phi_i(y). \tag{12}$$

By substituting the kernel expansion of Eq. (7) into Eq. (11), one gets

$$Z = \sum_i a_i^2 \lambda_i^{N-1}, \tag{13}$$

which is the counterpart of Eq. (10) for sequences with open ends. At that point, one is able to calculate all extensive thermodynamic quantities of finite sequences with open boundary conditions. For example, the free energy F, the entropy S, and the specific heat C_V are straightforwardly obtained from

$$F = -k_B T \ln(Z),$$

$$S = -\frac{\partial F}{\partial T},$$

$$C_V = -T \frac{\partial^2 F}{\partial T^2}. \tag{14}$$

Calculation of nonextensive quantities, like the average base pair separation $\langle y \rangle$ and the correlation length ξ, is more involved. $\langle y \rangle$ is the mean separation of the bases averaged over the sites of the sequence, that is,

$$\langle y \rangle = \frac{1}{N} \sum_{n=1}^{N} \langle y_n \rangle. \tag{15}$$

In order to reduce $\langle y_n \rangle$ to a form depending only on the eigenvalues and eigenvectors of the TI operator, it is first rewritten in the form

$$\langle y_n \rangle = \frac{1}{Z} \int dy_1 dy_2 \cdots dy_N y_n e^{-\beta V_M(y_1)/2} K(y_2, y_1) \times K(y_3, y_2) \cdots K(y_N, y_{N-1}) e^{-\beta V_M(y_N)/2}. \quad (16)$$

Substituting Eq. (7) into Eq. (16) and defining

$$b_i = \int dy\ e^{-\beta V_M(y)/2} \Phi_i(y) y,$$

$$Y_{ij}^{(1)} = \int dy\ \Phi_i(y) y \Phi_j(y), \quad (17)$$

one obtains

$$\langle y_1 \rangle = \langle y_N \rangle = \frac{1}{Z} \sum_i a_i b_i \lambda_i^{N-1} \quad (18)$$

and

$$\langle y_n \rangle = \frac{1}{Z} \sum_{i,j} a_i a_j Y_{ij}^{(1)} \lambda_i^{n-1} \lambda_j^{N-n} \quad (19)$$

for $n \neq 1, N$. By evaluating the geometric summation that appears in Eq. (15) when the $\langle y_n \rangle$ are replaced by their expressions in Eqs. (18) and (19), one finally gets

$$\langle y \rangle = \frac{2}{ZN} \sum_i a_i b_i \lambda_i^{N-1} + \frac{1}{ZN} \sum_{i,j} a_i a_j Y_{ij}^{(1)} \lambda_i^{-1} \lambda_j^N \frac{r_{ij}^2 - r_{ij}^N}{1 - r_{ij}} \quad (20)$$

where $r_{ij} = \lambda_i / \lambda_j$. Note that Eq. (19) was already obtained by Zhang *et al.* [35]. Equation (20) is the counterpart for finite sequences with open ends of the much simpler formula $\langle y \rangle = Y_{11}^{(1)}$, which was used in our preceding work [33] and applies only to infinitely long sequences.

The correlation length ξ is defined as

$$\xi^2 = - \left. \frac{1}{2S(q)} \frac{d^2 S(q)}{dq^2} \right|_{q=0}, \quad (21)$$

where $S(q)$ is the static form factor

$$S(q) = \left\langle \left| \sum_{n=1}^{N} (y_n - \langle y_n \rangle) e^{iqan} \right|^2 \right\rangle. \quad (22)$$

In this equation, a stands for the distance between successive base pairs. For infinitely long chains, one simply obtains $\xi = a / \ln(\lambda_1 / \lambda_2)$, where λ_2 is the second largest eigenvalue of the integral operator [34]. The calculation for finite sequences with open boundary conditions is more tricky. In order to separate explicitly the contributions of the base pairs at the extremities, Eq. (22) is first rewritten in the form

$$S(q) = \sum_{n=1}^{N} \sum_{m=1}^{N} \langle \delta y_n \delta y_m \rangle e^{iqa(n-m)}, \quad (23)$$

where $\delta y_n = y_n - \langle y_n \rangle$. By isolating averages concerning extremity values, one gets

$$S(q) = \langle \delta y_1^2 \rangle + \langle \delta y_N^2 \rangle + 2 \langle \delta y_1 \delta y_N \rangle \cos[qa(N-1)] + S_1 e^{iqa} + S_1^* e^{-iqa} + S_N e^{iNqa} + S_N^* e^{-iNqa} + S_{\text{mid}}, \quad (24)$$

where

$$S_1 = \sum_{m=2}^{N-1} \langle \delta y_1 \delta y_m \rangle e^{-iqam},$$

$$S_N = \sum_{m=2}^{N-1} \langle \delta y_m \delta y_N \rangle e^{-iqam},$$

$$S_{\text{mid}} = \sum_{m=2}^{N-1} \sum_{n=2}^{N-1} \langle \delta y_n \delta y_m \rangle e^{iqa(n-m)}. \quad (25)$$

Defining

$$c_i = \int dy\ e^{-\beta V_M(y)/2} y^2 \Phi_i(y),$$

$$Y_{ij}^{(2)} = \int dy\ \Phi_i(y) y^2 \Phi_j(y), \quad (26)$$

one obtains the relations

$$\langle y_1^2 \rangle = \langle y_N^2 \rangle = \frac{1}{Z} \sum_i a_i c_i \lambda_i^{N-1},$$

$$\langle y_1 y_N \rangle = \frac{1}{Z} \sum_i b_i^2 \lambda_i^{N-1},$$

$$\langle y_1 y_m \rangle = \frac{1}{Z} \sum_{ij} a_j b_i \lambda_i^{m-1} \lambda_j^{N-m} Y_{ij}^{(1)},$$

$$\langle y_m y_N \rangle = \frac{1}{Z} \sum_{ij} a_i b_j \lambda_i^{m-1} \lambda_j^{N-m} Y_{ij}^{(1)},$$

$$\langle y_n^2 \rangle = \frac{1}{Z} \sum_{ij} a_i a_j \lambda_i^{n-1} \lambda_j^{N-n} Y_{ij}^{(2)},$$

$$\langle y_n y_m \rangle = \frac{1}{Z} \sum_{ijk} a_i a_k Y_{ij}^{(1)} Y_{jk}^{(1)} \begin{cases} \lambda_i^{n-1} \lambda_j^{m-n} \lambda_k^{N-m} & \text{if } m > n, \\ \lambda_i^{m-1} \lambda_j^{n-m} \lambda_k^{N-n} & \text{if } m < n. \end{cases} \quad (27)$$

By evaluating analytically the geometric series which appear when Eq. (27) is substituted in Eqs. (24) and (25), one obtains after some tedious algebra the rather lengthy expression for $S(q)$ which is reported in the Appendix. According to Eq. (21), this expression must finally be differentiated twice with respect to the wave vector q in order to get the correlation length.

From a practical point of view, we used the procedure described in Appendix B of Ref. [34] to compute the eigenvalues and eigenvectors of the transfer integral operator in

Eq. (8). This procedure is based on the diagonalization of a matrix representation of the symmetric TI operator $K(x,y)$ defined on a grid of y values. For most calculations, we chose a grid consisting of 4201 y values regularly spaced between $y_{\min}=-200/A_M$ and $y_{\max}=4000/A_M$. Integrals were numerically evaluated on the same grid. Recall that the choice of a grid extending to very large values of y is crucial to get converged values of the various thermodynamic quantities [33,47]. In order to check the convergence of the results presented below, we performed some calculations on a larger grid consisting of 6201 y values regularly spaced between $y_{\min}=-200/A_M$ and $y_{\max}=6000/A_M$. We will come back later to this point.

Moreover, in the thermodynamic limit $N\to\infty$ the major contribution to the partition function arises from the largest eigenvalue λ_1 and in this limit it is reasonable to drop eigenvalues λ_i with $i\geq 2$. However, this work considers large DNA molecules as well as smaller ones. Consequently, as many eigenvalues as possible must be taken into account in the practical evaluation of Eqs. (13) and (20) and the expression for $S(q)$ in the Appendix. Still, it was found that the contribution of eigenvalues beyond the first 400 largest ones is completely negligible.

In addition to the two caveats above, it should, of course, be recalled that the results of the TI method become questionable when the last bound state disappears, that is, above the melting temperature [35].

IV. FINITE SIZE EFFECTS NEAR THE CRITICAL POINT

A. Rounding of the melting transition of DNA

It is well known that a finite size system does not exhibit any phase transition. At the critical point its free energy is analytic and consequently all thermodynamic quantities are regular. Let L be the size of a system having a critical behavior in the thermodynamic limit $L\to\infty$. For this system, finite size effects manifest themselves as $e^{-L/\xi}$, where ξ is the correlation length, by rounding the critical point singularity. In other words, these effects become important over a region for which $\xi\sim L$. A simple description of the rounding phenomena which take place in the Ising model can be found in Ref. [48]. For an infinite size Ising system, the order parameter jumps discontinuously from $-M_{\rm cr}$ to $+M_{\rm cr}$ as the applied magnetic field H is increased and crosses the critical value $H=0$. On the other hand, if the system's size is finite, this transition occurs on a finite region of order $\Delta H \simeq k_BT/(M_{\rm cr}L^d)$ with a large but finite slope $\sim M_L^2L^d/(k_BT)$, where d is the dimensionality and M_L the most probable value of the magnetization of the finite system.

For the two DNA models sketched in Sec. II, the size L of the system is equal to the number N of base pairs in the sequence times the distance between two successive base pairs. This latter quantity plays no role in the dynamics of the investigated models, so we will henceforth use N or L indiscriminately to refer to the size of the sequence.

Given a sequence of length N, the first task consists in determining its critical temperature, which we denote by $T_c(N)$. Among the several methods listed, for example, in Ref. [49], we found it rather simple and convenient to search for the maximum of the specific heat C_V, which is more pronounced than that of the correlation length ξ and therefore allows for a more accurate localization of the temperature. Two observations confirm *a posteriori* that the critical temperatures thus obtained are correct. First, the shift in critical temperature is found to vary as $1/N$, as predicted by finite size scaling theory and observed in experiments. The top plot of Fig. 1 shows, for example, the evolution of $1-T_c(N)/T_c$ as a function of N, where T_c stands for $T_c(\infty)$ (for the grid consisting of 4201 y values regularly spaced between $y_{\min}=-200/A_M$ and $y_{\max}=4000/A_M$, T_c is equal to 281.40 K for the DPB model and 367.63 K for the JB model). Open symbols denote the results of TI calculations, while straight lines show power laws adjusted against the TI results. The slopes of these power laws, $N^{-1.00}$ for the DPB model and $N^{-1.05}$ for the JB model, are in excellent agreement with the N^{-1} dependence predicted by finite size scaling theory and observed in experiments. Note, however, that the absolute deviations are too large by a factor of 4 for the DPB model and 6.5 for the JB model, compared to the $T_c-T_c(N)=500/N$ dependence which is plugged into online oligonucleotide property calculators. One could probably adjust the parameters of each model slightly to decrease the magnitude of the prefactors of the power laws and get a better agreement between calcu-

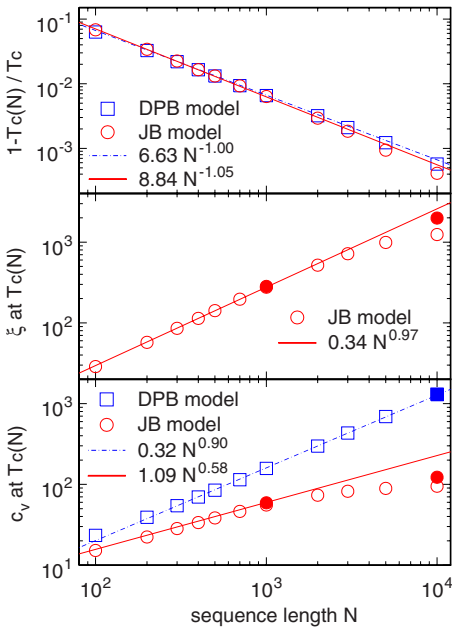

FIG. 1. (Color online) Log-log plots, as a function of the sequence length N, of the reduced critical temperature shift $1-T_c(N)/T_c(\infty)$ (top plot), the value of the correlation length ξ at $T_c(N)$ (middle plot), and the value of the specific heat c_V at $T_c(N)$ (bottom plot). ξ is in units of the separation between two successive base pairs, and c_V in units of k_B. Squares and circles show the results obtained with the TI method for the DPB and JB models, respectively. Open symbols denote results obtained with grids of 4201 y values, while the few filled symbols denote results obtained with larger grids of 6201 y values (see end of Sec. IV A). The solid and dash-dotted lines show the results of the adjustment of power laws against the calculated points.

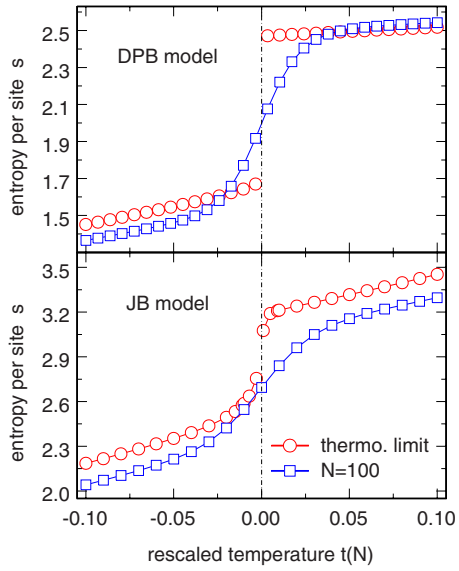

FIG. 2. (Color online) Entropy per site s as a function of the rescaled temperature $t(N)$ for an infinitely long chain (circles) and a sequence with $N=100$ basepairs (squares), according to the DPB (top plot) and the JB models (bottom plot). s is in units of k_B.

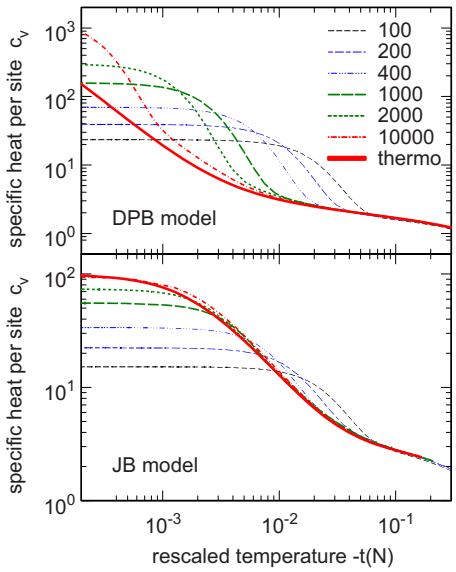

FIG. 3. (Color online) Log-log plots of the specific heat per site c_V as a function of the negative $-t(N)$ of the rescaled temperature for the DPB (top plot) and the JB models (bottom plot), and seven values of the sequence length N ranging from 100 to ∞. c_V is in units of k_B. Note that, at the thermodynamic limit of infinitely long chains, c_V becomes infinite at the critical temperature, but numerical limitations of the TI method prevent the observation of such divergence.

lated and measured deviations of the critical temperature, but we made no attempt in this direction. The validity of the method we used to determine $T_c(N)$ is further demonstrated, as will be seen later in this section, by the fact that the curves for the temperature evolution of C_V, ξ, $\langle y \rangle$, etc., for sequences with different lengths N, all coincide sufficiently far from the critical temperature when plotted as a function of the reduced temperature

$$t(N) = \frac{T - T_c(N)}{T_c(N)}. \tag{28}$$

In order to illustrate finite size effects on DNA melting, we first computed the entropy per base, $s=S/N$, for an infinite chain and a short DNA sequence for both the DPB and the JB models. Results are shown in Fig. 2. At the thermodynamic limit, the entropy s is clearly singular at the critical temperature, as is expected for first-order phase transitions. In contrast, smooth curves are observed over the whole temperature range for a sequence with $N=100$. Note that the singularities observed in Fig. 2 for infinitely long chains are not steps but true divergences. s indeed diverges as $(T_c - T)^{1-\alpha}$, where α, the critical exponent of the specific heat per base $c_V=C_V/N$, is slightly but significantly larger than 1 for both models (α is equal to 1.45 for the DPB model and 1.13 for the JB model [33]). The reason that the singularities look like steps instead of divergences is simply that the divergences are quite slow, so that in the interval of $t(N)$ values where the TI method works s diverges by an amount substantially smaller than the gap between the two asymptotic straight lines.

We next computed the specific heat per base c_V for increasing sequence length and temperature. The top and bottom plots of Fig. 3 show the temperature evolution of c_V for seven values of N ranging from 100 to infinity for the DPB and JB models, respectively. It is seen in this figure that rounding manifests itself through a decrease in the maximum of c_V as N decreases, but also through the fact that the sharp rise of c_V takes place further and further from the critical temperature, that is, at increasingly larger values of $|t(N)|$. This is particularly clear for the DPB model, which at the thermodynamic limit undergoes a very sharp transition, i.e., a transition that is noticeable only at very small values of $|t| = |t(\infty)|$ [33]. Quite interestingly, examination of Fig. 3 also indicates that the two models consequently give very comparable results up to $N \simeq 1000$, while the narrower nature of the phase transition for the DPB model becomes apparent for longer sequences.

We also computed, for the JB model, the temperature evolution of the correlation length ξ [according to Eq. (21) and the expression for $S(q)$ in the Appendix] for increasing values of N. For a finite system, the value of ξ at $T_c(N)$ is expected to be of the order of magnitude of the finite length of the system and to increase as N. This behavior can be checked in the middle plot of Fig. 1, which shows the evolution of ξ at $T_c(N)$ (in units of the separation between successive base pairs) as a function of N: ξ is indeed of the same order of magnitude as N and the curve scales as $N^{0.97}$. An exception, however, occurs for the last three points with $N \geq 3000$: we will come back to this point at the end of this section. The bottom plot of Fig. 4 additionally shows the temperature evolution of ξ for seven values of N ranging from 100 to infinity. One observes just the same rounding effects as for the specific heat in Fig. 3.

We finally computed, for the JB model, the temperature evolution of the average base pair separation $\langle y \rangle$ [according

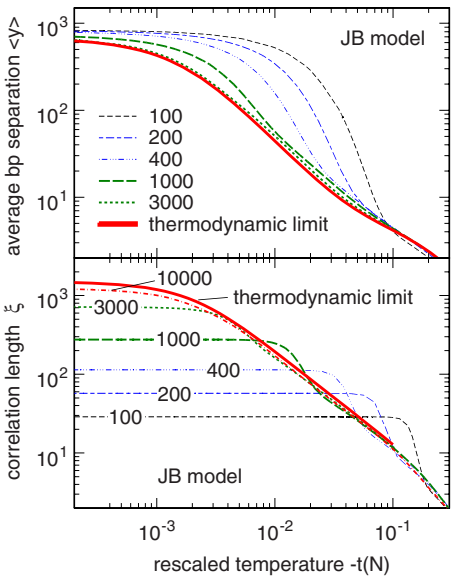

FIG. 4. (Color online) Log-log plots of the correlation length ξ (bottom plot) and the average base pair separation $\langle y \rangle$ (top plot) as a function of the negative $-t(N)$ of the rescaled temperature for the JB model and seven values of the sequence length N ranging from 100 to ∞. ξ is in units of the separation a between two successive base pairs and $\langle y \rangle$ in units of the inverse $1/A_M$ of the Morse potential parameter. Note that, at the thermodynamic limit of infinitely long chains, ξ and $\langle y \rangle$ become infinite at the critical temperature, but numerical limitations of the TI method prevent the observation of such divergence.

to Eq. (20)] for increasing values of N. The result is shown in the top plot of Fig. 4. Although the same rounding effect is observed as for the specific heat c_V (Fig. 3) and the correlation length ξ (bottom plot of Fig. 4), this latter plot displays the remarkable feature that for very small $t(N)$ all curves seem to converge to the same limit, which is the approximation of infinity imposed by the numerical limitations of the TI method.

Before concluding this section, let us have a closer look at the precision of TI calculations. As already mentioned at the end of Sec. III, this precision depends crucially on the size and extension of the grid of y values that is used to diagonalize the TI kernel and compute the various integrals [33]. The TI method fails to give correct values of thermodynamic observables too close to the phase transition discontinuity, but the broader the extension of the grid, the closer one can approach the discontinuity with TI calculations. While all calculations presented so far were obtained with a grid consisting of 4201 y values regularly spaced between $y_{\min}=-200/A_M$ and $y_{\max}=4000/A_M$, we performed some calculations with a larger grid consisting of 6201 y values regularly spaced between $y_{\min}=-200/A_M$ and $y_{\max}=6000/A_M$ in order to check the precision of these results. The values obtained with the broader grid are shown as filled symbols in the two bottom plots of Fig. 1, which display the evolution with the sequence length N of the values at $T_c(N)$ of the correlation length ξ and the specific heat c_V [note that these are the two quantities that are most sensitive to the convergence of TI calculations because they are calculated at $T_c(N)$]. It is seen that results appear to be already converged with the smallest grid for the DPB model up to $N=10\,000$, while for the JB model convergence at $T_c(N)$ is still poor for N larger than a few thousands. Note that this is rather reassuring, since this is precisely the range of values of N for which values calculated with the JB model depart from the power laws indicated by straight lines. This is also in excellent agreement with Figs. 3 and 4, which show that sequences of length $N=10\,000$ are still rather far from the thermodynamic limit for the DPB model, so that one need not worry about the effect of the discontinuity on TI calculations, while in contrast sequences with a few thousands of base pairs are already close to the thermodynamic limit for the JB model, so that the perturbative effect of the discontinuity becomes noticeable in TI calculations.

B. Finite size scaling analysis

The basic idea of finite size scaling is that the correlation length ξ is the only length that matters close to the critical temperature and that one just needs to compare the linear dimension L of the system to ξ: rounding and shifting indeed set in as soon as $L/\xi \sim 1$. By definition of the critical exponent ν, ξ grows as $|t|^{-\nu}$ in the limit of large L values. In this limit, (L/ξ) is therefore proportional to $|t|^{\nu}L$, that is, to a power of $|t|L^{1/\nu}$ or equivalently of $|t|N^{1/\nu}$. In the absence of an external field, it is therefore natural to write the singular part of the free energy of the finite size system in the form

$$f_{\text{sing}} = N^{-d} Y(|t|N^{1/\nu}), \tag{29}$$

where Y is some homogeneous function. Differentiating Eq. (29) twice with respect to t, one obtains that c_V is equal to

$$c_V = N^{\rho} G(|t|N^{\sigma}), \tag{30}$$

where

$$\rho = \frac{2}{\nu} - d,$$

$$\sigma = \frac{1}{\nu}, \tag{31}$$

and G is a homogeneous function that is proportional to the second derivative of Y. By using Josephson's identity $2-\alpha = \nu d$, where α is the critical exponent for c_V ($c_V \propto |t|^{-\alpha}$), the coefficients ρ and σ can be recast in the forms

$$\rho = \frac{\alpha}{\nu},$$

$$\sigma = \frac{1}{\nu}. \tag{32}$$

Note that Eq. (32) is often preferred to Eq. (31) in general presentations of finite size scaling theory [see, for example, Eq. (1.7) of Ref. [50]].

In order to tackle the more complex case where several lengths diverge at the critical point, as is the case for DNA melting, Binder *et al.* [51] derived a method that is based on

TABLE I. Values of the coefficients ρ and σ of Eq. (30) for the DPB and JB models. The first three lines show the values calculated from the critical exponents reported in Table I of Ref. [33] and Eqs. (31), (32), and (34). The last line shows the values adjusted by hand in order that the plots of c_V/N^ρ as a function of tN^σ are superposed over an interval of values of N as large as possible (see bottom plots of Figs. 5 and 6). The confidence intervals shown in parentheses were obtained, for calculated values of ρ and σ, by assuming additive 5% uncertainties in the values of the critical exponents reported in Ref. [33]. The confidence intervals for the adjusted values are more subjective. They were deduced from visual inspection of c_V/N^ρ versus tN^σ plots.

	DPB model		JB model	
	ρ	σ	ρ	σ
Eq. (31)	0.79 (0.70–0.88)	0.89 (0.85–0.94)	0.63 (0.55–0.71)	0.81 (0.77–0.85)
Eq. (32)	1.29 (1.17–1.43)	0.89 (0.85–0.94)	0.92 (0.83–1.02)	0.81 (0.77–0.85)
Eq. (34)	1.78 (1.04–3.25)	1.39 (1.03–2.11)	1.82 (0.98–3.84)	1.41 (0.99–2.42)
Adjusted	0.85 (0.80–0.90)	1.00 (0.98–1.02)	0.45 (0.35–0.55)	0.90 (0.85–0.95)

the use of an irrelevant variable u and an expression of the form

$$f_{\text{sing}} = N^{-d} F(tN^{y_t}, uN^{y_u}). \tag{33}$$

After several approximations and a little bit of algebra, these authors obtain c_V in the form of Eq. (30) with, however,

$$\rho = \frac{2d}{2\beta + \gamma} - d,$$

$$\sigma = \frac{d}{2\beta + \gamma}, \tag{34}$$

where β and γ are the critical exponents for the order parameter m ($m \sim |t|^\beta$) and its derivative with respect to the applied external field ($dm/dh \sim |t|^{-\gamma}$), respectively.

Table I shows the values of ρ and σ calculated from the characteristic exponents reported in Table I of Ref. [33] and Eqs (31), (32), and (34), as well as adjusted values. These latter were obtained by varying ρ and σ by hand in order that the plots of c_V/N^ρ as a function of tN^σ are superposed for an interval of values of N as large as possible. By setting $t=0$ in Eq. (30), one sees that the value of c_V at $T_c(N)$ scales as N^ρ. ρ was therefore adjusted in the neighborhood of the slope of the plot of the value of c_V at $T_c(N)$ as a function of N (bottom plot of Fig. 1). On the other hand, σ was adjusted in the neighborhood of $1/\nu$. The confidence intervals shown in parentheses in Table I were obtained, for calculated values of ρ and σ, by assuming additive 5% uncertainties in the values of the critical exponents reported in Table I of Ref. [33]. The confidence intervals for the adjusted values are more subjective. They were deduced from visual inspection of c_V/N^ρ versus tN^σ plots. Examination of Table I indicates that the values of ρ and σ obtained from Eq. (31) compare well with the adjusted ones, while this is certainly not the case for the values obtained from Eqs. (32) and (34). Figures 5 and 6 further show plots of c_V/N^ρ as a function of tN^σ for, respectively, the DPB and JB models, and values of ρ and σ obtained from Eq. (32) (top plots) and adjusted ones (bottom plots). It is seen in the top plots that the curves with different values of N are far from being superposed for the values of ρ and σ obtained from Eq. (32), and the situation is still worse with Eq. (34). In contrast, the various curves are fairly well superposed for the adjusted values of ρ and σ (see bottom plots of Figs. 5 and 6), as well as those obtained with Eq. (31). For the JB model, an exception occurs for the curve corresponding to $N=10\,000$ (bottom plot of Fig. 6). As discussed in some detail in the last paragraph of Sec. IV A, TI calculations applied to the JB model are not sufficiently converged for sequences with more than a few thousand base pairs, which could explain why the curve for $N=10\,000$ does not align with the other ones.

The fact that Eq. (31) leads to a correct superposition of the curves for different values of the sequence length N is the proof that the basic hypothesis of finite size scaling theory is satisfied. On the other hand, the fact that curves with different N are no longer superposed when Eq. (32) is used to calculate ρ and σ simply reflects the fact that Josephson's

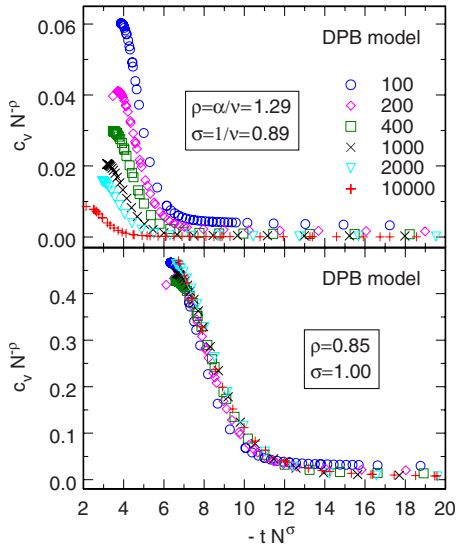

FIG. 5. (Color online) c_V/N^ρ, for six values of the sequence length N ranging from 100 to 10 000, as a function of $-tN^\sigma$ for the DPB model and values of ρ and σ obtained from Eq. (32) (top plot) or adjusted by hand (bottom plot).

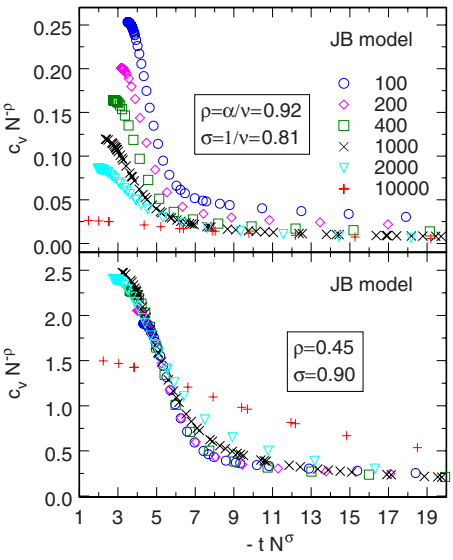

FIG. 6. (Color online) c_V/N^{ρ}, for six values of the sequence length N ranging from 100 to 10 000, as a function of $-tN^{\sigma}$ for the JB model and values of ρ and σ obtained from Eq. (32) (top plot) or adjusted by hand (bottom plot).

identity $2-\alpha=\nu d$ is not valid for these two models of DNA melting, as clearly shown in Table II of Ref. [33]. Finally, the fact that the curves also do not superpose when Eq. (34) is used indicates that one of the several hypotheses made by the authors of Ref. [51] to arrive at these expressions is not satisfied for the DNA models, although it is not an easy task to tell which one(s) is (are) invalidated. Alternatively, Eq. (34) can be straightforwardly derived from Eq. (31) by using the Rushbrooke identity $(\alpha+2\beta+\gamma=2)$ as well as the Josephson one. Since this latter identity is not valid, it comes as no surprise that Eq. (34) leads to as poor a result as Eq. (32).

V. CONCLUSION

To summarize, we modified the transfer integral method to adapt it to the calculation of thermodynamic quantities of finite sequences with open boundary conditions. Nonextensive quantities, like the average separation of paired bases $\langle y\rangle$ and the correlation length ξ, turned out to be the trickiest ones to evaluate. We then applied this modified procedure to the DPB and JB dynamical models, in order to clarify how the finiteness of the length of the sequence affects the phase transition that takes place at the DNA melting temperature. We showed that the rounding of the transition that occurs when the size of the sequence decreases is clearly reflected in the temperature evolution of most quantities, including the specific heat c_V, the correlation length ξ, and the average separation of paired bases $\langle y\rangle$. We next performed a finite size scaling analysis of the two systems and showed that the singular part of the free energy can indeed be expressed in terms of a homogeneous function. However, Josephson's identity is satisfied for none of the investigated systems, so that the derivation of the characteristic exponents ρ and σ, which appear in the asymptotic expression of the specific heat c_V, requires some care.

The transfer integral method appears to be the only efficient numerical tool to study the thermodynamics of DNA melting in detail. In the formulation used here, however, it applies only to homogeneous chains, while it is well established that the heterogeneity of real DNA molecules may smear out the discontinuity of the melting transition, just as the finiteness of the sequence does. Our next goal is therefore to overcome the technical difficulty associated with the application of the TI method to inhomogeneous chains and investigate the effect of heterogeneities on the phase transition at DNA melting.

APPENDIX: EXPRESSION FOR THE STATIC FORM FACTOR

The expression we obtained for the static form factor $S(q)$ is

$$S(q) = \langle \delta y_1^2 \rangle + \langle \delta y_N^2 \rangle + 2\langle \delta y_1 \delta y_N \rangle \cos[qa(N-1)] + \sum_{ij} H_{ij} \frac{f_{ij}(2) - f_{ij}(N)}{1 - f_{ij}(1)} + \sum_{i,j} \frac{1}{\cosh(\alpha_{ij}) - \cos(qa)} \{[D_{ij} f_{ij}(1) + C_{ij} f_{ij}(N)]$$
$$\times \cos[(N-2)qa] - D_{ij} f_{ij}(N-1) - C_{ij} f_{ij}(2) - [D_{ij} f_{ij}(2) + C_{ij} f_{ij}(N-1)] \cos[(N-1)qa] + [D_{ij} f_{ij}(N) + C_{ij} f_{ij}(1)]$$
$$\times \cos[qa]\} + \sum_{ijk} \frac{2M_{ijk}}{[1 - g(1,1)][1 + f_{ij}(2) - 2f_{ij}(1)\cos(qa)][1 + f_{jk}(2) - 2f_{jk}(1)\cos(qa)]} \times \{-g(3,3) - g(4,4) - g(2,4)$$
$$+ g(N,N) + g(N,N+2) + g(N+1,N+1) + [g(2,3) - g(N,N+1) + 2g(3,4) - g(N+1,N+2) + g(4,3) - g(N+1,N)$$
$$- g(N,N+1)] \cos(qa) + [g(N+1,N+1) - g(3,3)] \cos(2qa) + [g(2,N+1) - g(3,N+2)] \cos[(N-3)qa] + [g(4,N+2)$$
$$- g(2,N)] \cos[(N-2)qa] + [g(3,N) - g(4,N+1)] \cos[(N-1)qa]\} + \left| \sum_{ij} M_{ij} \frac{e^{2(iqa-\alpha_{ij})} - e^{N(iqa-\alpha_{ij})}}{1 - e^{iqa-\alpha_{ij}}} \right|^2,$$

where

$$\alpha_{ij} = -\ln(r_{ij}),$$

$$M_{ij} = \frac{1}{Z}\lambda_i^{-1}\lambda_j^N a_i a_j Y_{ij}^{(1)},$$

$$H_{ij} = \frac{1}{Z}\lambda_i^{-1}\lambda_j^N a_i a_j Y_{ij}^{(2)},$$

$$T_{ij} = \frac{1}{Z}\lambda_i^{-1}\lambda_j^N b_i a_j Y_{ij}^{(1)},$$

$$G_{ij} = \frac{1}{Z}\lambda_i^{-1}\lambda_j^N a_i b_j Y_{ij}^{(1)},$$

$$C_{ij} = T_{ij} - \langle y_1 \rangle M_{ij},$$

$$D_{ij} = G_{ij} - \langle y_1 \rangle M_{ij},$$

$$f_{ij}(n) = e^{-n\alpha_{ij}},$$

$$g(n,m) = e^{-n\alpha_{ij} - m\alpha_{jk}}.$$

[1] A. Proykova and R. S. Berry, Z. Phys. D **40**, 215 (1997).
[2] O. G. Mouritsen, *Computer Studies of Phase Transitions and Critical Phenomena* (Springer-Verlag, Berlin, 1984).
[3] D. H. E. Gross, A. Ecker, and X. Z. Zhang, Ann. Phys. **5**, 446 (1996).
[4] D. H. E. Gross, M. E. Madjet, and O. Shapiro, Z. Phys. D **39**, 75 (1997).
[5] D. H. E. Gross and E. Votyakov, Eur. Phys. J. B **15**, 115 (2000).
[6] P. Borrmann, O. Mülken, and J. Harting, Phys. Rev. Lett. **84**, 3511 (2000).
[7] O. Mülken, P. Borrmann, J. Harting, and H. Stamerjohanns, Phys. Rev. A **64**, 013611 (2001).
[8] O. Mülken and P. Borrmann, Phys. Rev. C **63**, 024306 (2001).
[9] W. Janke and R. Kenna, J. Stat. Phys. **102**, 1211 (2001).
[10] R. B. Inman and R. L. Baldwin, J. Mol. Biol. **8**, 452 (1964).
[11] R. M. Wartell and A. S. Benight, Phys. Rep. **126**, 67 (1985).
[12] J. SantaLucia and D. Hicks, Annu. Rev. Biophys. Biomol. Struct. **33**, 415 (2004).
[13] I. E. Scheffler, E. L. Elson, and R. L. Baldwin, J. Mol. Biol. **48**, 145 (1970).
[14] J.-R. Sarasua, R. E. Prud'homme, M. Wisniewski, A. Le Borgne, and N. Spassky, Macromolecules **31**, 3895 (1998).
[15] M. Kuwahara, M. Arimitsu, M. Shigeyasu, N. Saeki, and M. Sisido, J. Am. Chem. Soc. **123**, 4653 (2001).
[16] D. De Luchi, C. Gouyette, and J. A. Subirana, Anal. Biochem. **322**, 279 (2003).
[17] K. J. Breslauer, R. Frank, H. Blöcker, and L. A. Marky, Proc. Natl. Acad. Sci. U.S.A. **83**, 3746 (1986).
[18] J. G. Duguid, V. A. Bloomfield, J. M. Benevides, and G. J. Thomas, Biophys. J. **71**, 3350 (1996).
[19] R. M. Myers, S. G. Fischer, T. Maniatis, and L. S. Lerman, Nucleic Acids Res. **13**, 3111 (1985).
[20] J. Zhu and R. M. Wartell, Biochemistry **36**, 15326 (1997).
[21] A. M. Paiva and R. D. Sheardy, Biochemistry **43**, 14218 (2004).
[22] S. Amrane, B. Saccà, M. Mills, M. Chauhan, H. H. Klump, and J.-L. Mergny, Nucleic Acids Res. **33**, 4065 (2005).
[23] Y. Zeng, A. Montrichok, and G. Zocchi, Phys. Rev. Lett. **91**, 148101 (2003).
[24] Y. Zeng, A. Montrichok, and G. Zocchi, J. Mol. Biol. **339**, 67 (2004).
[25] S. Ares, N. K. Voulgarakis, K. O. Rasmussen, and A. R. Bishop, Phys. Rev. Lett. **94**, 035504 (2005).
[26] T. S. van Erp, S. Cuesta-Lopez, and M. Peyrard, Eur. Phys. J. E **20**, 421 (2006).
[27] T. Dauxois, M. Peyrard, and A. R. Bishop, Phys. Rev. E **47**, R44 (1993).
[28] M. Peyrard and A. R. Bishop, Phys. Rev. Lett. **62**, 2755 (1989).
[29] M. Joyeux and S. Buyukdagli, Phys. Rev. E **72**, 051902 (2005).
[30] R. D. Blake, J. W. Bizzaro, J. D. Blake, G. R. Day, S. G. Delcourt, J. Knowles, K. A. Marx, and J. SantaLucia, Bioinformatics **15**, 370 (1999).
[31] M. Barbi, S. Lepri, M. Peyrard, and N. Theodorakopoulos, Phys. Rev. E **68**, 061909 (2003).
[32] S. Buyukdagli, M. Sanrey, and M. Joyeux, Chem. Phys. Lett. **419**, 434 (2006).
[33] S. Buyukdagli and M. Joyeux, Phys. Rev. E **73**, 051910 (2006).
[34] T. Schneider and E. Stoll, Phys. Rev. B **22**, 5317 (1980).
[35] Y. L. Zhang, W. M. Zheng, J. X. Liu, and Y. Z. Chen, Phys. Rev. E **56**, 7100 (1997).
[36] N. Theodorakopoulos, T. Dauxois, and M. Peyrard, Phys. Rev. Lett. **85**, 6 (2000).
[37] M. E. Fisher and M. N. Barber, Phys. Rev. Lett. **28**, 1516 (1972).
[38] H. W. J. Blöte and E. Luijten, Europhys. Lett. **38**, 565 (1997).
[39] E. Luijten, K. Binder, and H. W. J. Blöte, Eur. Phys. J. B **9**, 289 (1999).
[40] Z. Merdan and R. Erdem, Phys. Lett. A **330**, 403 (2004).
[41] S. Clar, B. Drossel, K. Schenk, and F. Schwabl, Phys. Rev. E **56**, 2467 (1997).
[42] M. Masihi, P. R. King, and P. Nurafza, Phys. Rev. E **74**, 042102 (2006).
[43] D. Poland and H. R. Scheraga, *Theory of Helix Coil Transition in Biopolymers* (Academic Press, New York, 1970).
[44] A. S. Benight, D. K. Howell, and R. M. Wartell, Nature (London) **289**, 203 (1981).
[45] A. Campa and A. Giansanti, J. Biol. Phys. **24**, 141 (1999).
[46] R. Owczarzy, P. M. Vallone, F. J. Gallo, T. M. Paner, M. J. Lane, and A. S. Benight, Biopolymers **44**, 217 (1997).
[47] N. Theodorakopoulos, Phys. Rev. E **68**, 026109 (2003).

[48] K. Binder and D.P. Landau, Phys. Rev. B **30**, 1477 (1984).
[49] K. Binder, Ferroelectrics **73**, 43 (1987).
[50] V. Privman, in *Finite Size Scaling and Numerical Simulation of Statistical Systems*, edited by V. Privman (World Scientific, Singapore, 1990), p. 8.
[51] K. Binder, M. Nauenberg, V. Privman, and A. P. Young, Phys. Rev. B **31**, 1498 (1985).